Polymer Bulletin (2021) 78:2155–2175
https://doi.org/10.1007/s00289-020-03207-2

ORIGINAL PAPER

Studies on favorable ionic conduction and structural properties of biopolymer electrolytes system-based alginate

A. F. Fuzlin[1] · **A. S. Samsudin**[1]

Received: 26 January 2019 / Revised: 18 March 2020 / Accepted: 16 April 2020 / Published online: 29 April 2020

Abstract

In this present work, the investigation of solid biopolymer electrolytes (SBEs)-based alginate-doped NH_4Br was carried out and prepared via casting technique. The SBEs system was characterized using Fourier transform infrared, thermal gravimetric analysis, differential scanning calorimetry, X-ray diffraction, scanning electron microscope, and electrical impedance spectroscopy. Based on IR-analysis, it was shown that the complexation between alginate and NH_4Br has occurred based on the changes of peak at COO^- group of alginate. The interaction led to the improvement in amorphous phase and thermal stability of SBEs system when NH_4Br was added. The ionic conductivity of SBEs system was found to achieve maximum value at 4.41×10^{-5} S/cm when 20 wt. % of NH_4Br was added and the value was comparable with other types of polymer electrolytes system. The temperature-dependence ionic conductivity of entire SBEs system obeys Arrhenius behavior where the $R^2 \sim 1$ and present system are thermally assisted. From IR-deconvolution approach, it can be found that the ionic conductivity of alginate-NH_4Br SBEs system was governed by ions mobility, μ and diffusion coefficient, D. All these findings imply that present alginate-based SBEs system is potential to be applied in electrochemical devices, i.e., proton battery, supercapacitor and fuel cell.

Keywords Alginate · Ionic conductivity · Protonation · Deconvolution technique · Transport properties

✉ A. S. Samsudin
ahmadsalihin@ump.edu.my

[1] Ionic Materials Team, Faculty of Industrial Sciences and Technology, Universiti Malaysia Pahang, 26300 Pahang, Malaysia

Introduction

Nowadays, energy storage or electrochemical device turns out to be the current attraction around the world where the development of energy devices enlightening the area of technology industry. Solar cell, supercapacitor, battery, fuel cell and monochromic device are the main example of energy device [1]. Electrolyte is identified one of the important components in the electrochemical device by operating the transference of ionic charges between electrolyte–electrode interfaces through the charge–discharge process; hence, the electricity will be conduct [2]. Liquid electrolytes (LE) were well known used in electrochemical devices due to good ionic conductivity [3]. However, there are problems reported using LE making it less suitable for energy device applications including harmful, leakage, poor electrochemical stability, high-cost and non-biodegradable [4, 5]. In order to overcome these drawbacks, solid biopolymer electrolyte has been studied widely. Biomaterials are one of the interests in the development of electrochemical devices as they are biodegradable and derived from renewable sources for promising performance.

Biomaterial is from natural resources, which are leakage-free, abundant in nature, low-cost production and good mechanical properties [6–9]. Many research has been conducted based on biopolymer for electrolytes application such as chitosan [10], carboxymethyl cellulose (CMC) [11], corn-starch [12], carrageenan [13], pectin [14] and agarose [15], and when doping with appropriate dopant, the conduction properties enhance in the ranging from 10^{-6} to 10^{-4} S cm^{-1}. Alginate is another example of bio-polymer which suitable as an application for biopolymer electrolytes. In general, alginate is linear polysaccharides derived from a family of carbohydrates, which is origin of brown algae, and it is water soluble as a natural polymer [16–18]. The alginate was suitably used in polymer electrolytes due to the presence of carboxyl group, which could enhance the conduction performance. One of the alternatives in the electrochemical properties is via incorporation of dopant. In polymer electrolytes system, ionic dopant is dispersed in polymer backbone to generate ion conduction by acting as ionic charge carriers. Various types of ionic dopant have been thoroughly studied, including ammonium bromide (NH_4Br) where it is classified as one of the charge carrier's donors with excellent ability to donate proton (H^+) and responsible for improving the ionic conduction of SBEs system [19–21].

It is an effort to reduce dependency on petrochemical-based electrolytes; therefore, this present work focuses on development of biopolymer namely alginate, which acts as host polymer and doped with ammonium bromide (NH_4Br) as a possibility to become new type of polymer electrolytes system. The prepared sample was analyzed for structural and conduction properties by using Fourier transform infrared (FTIR) spectroscopy, thermal gravimetric analysis (TGA), differential scanning calorimetry (DSC), X-ray diffraction (XRD), scanning electron microscope (SEM) and electrical impedance spectroscopy (EIS), respectively.

Materials and methods

Materials

Biomaterial namely alginate (M.W. ~ 40,000) was obtained from Shaanxi Orient Co. and ammonium bromide, NH_4Br (MW: 97.94 g mol^{-1}) from Merck Co., respectively. In the present work, distilled water was used as solvent to dissolve alginate and NH_4Br.

Sample preparation

2 g of alginate is dissolved in distilled water. Then, various amounts of NH_4Br composition (5–30 wt. %) were added into alginate solution and stirred continuously until obtain a homogeneous mixture. The obtained mixture of alginate–NH_4Br was poured into a petri dish and subjected in the oven (55 °C for 7 h) for drying process to obtain film form. The prepared samples were left in desiccator (with silica gel) for further drying in order to avoid any solvent trapped in the present sample. The designation of entire samples was tabulated in Table 1.

Fourier transforms infrared spectroscopy (FTIR)

For the interaction analysis for alginate-NH_4Br SBEs system, Fourier transform infrared (FTIR) spectroscopy using Perkin Elmer 100 spectroscopy was carried out using attenuated total reflection (ATR) accessory with germanium crystal. The sample was placed on germanium crystal, and infrared light was passed through the sample within the frequency from range 4000 to 700 cm^{-1} with resolution of 2 cm^{-1}.

Thermal gravimetric analysis (TGA)

The thermal stability of the solid biopolymer electrolytes (SBEs) system was carried out by using Mettle Toledo TGA-DSC. The weight of sample was measured around ~ 2 mg and put into the silica crucible. The sample was heated up in range

Table 1 Description of the alginate-NH_4Br in SBE system

Description	NH_4Br (wt. %)
AlAB-0	0
AlAB-1	5
AlAB-2	10
AlAB-3	15
AlAB-4	20
AlAB-5	25
AlAB-6	30

30–800 °C with the heating rate of 10 °C min^{-1}. The measurements were recorded in a nitrogen gas atmosphere at a flow rate of 20 ml min^{-1}.

Differential scanning calorimetry (DSC)

The thermal properties of the prepared SBEs were determined by using NETZSCH DSC 214 polyma model where the prepared sample was sealed in an aluminum pan. The glass transition (T_g) of SBEs was analyzed at a heating rate of 10 °C min^{-1} in the temperature range from 30 to 300 °C under 40 mL min^{-1} flow of nitrogen inert atmosphere.

X-ray diffraction (XRD)

XRD profiles of alginate-NH_4Br samples were recorded by using Rigaku MiniFlex II diffractometer at ambient temperature. The suitable size sample was adhered onto a sample holder. The spectra of XRD were scanned using C_uK_α ($\lambda = 1.5406$ Å) radiation in the Bragg angle 2θ range from 5° to 80°.

Scanning electron microscope (SEM)

The surface morphological analysis of the SBEs system at ambient temperature was investigated using FEI quanta 450 scanning electron microscope (SEM) with an accelerating voltage of 10 kV. SEM characterization was carried out at 2000-× magnification by using Everhart Thornley detector (ETD).

Electrical impedance spectroscopy (EIS)

Ionic conductivity of alginate-NH_4Br SBEs system was characterized using impedance spectroscopy from HIOKI 3532-50 LCR Hi–Tester from ambient temperature to 353 K in the frequency range from 50 Hz to 1 MHz. The ionic conductivity, σ, of the film electrolyte was calculated using the following equation:

$$\sigma = \frac{b}{R_b A} \tag{1}$$

where b is the thickness of the electrolytes (cm), R_b is bulk resistance (Ω) and A is the electrode–electrolyte contact area (cm^2).

Transport parameter analysis

The FTIR deconvolution approach is used in order to determine the free ions and transport properties of SBEs system using Origin Lab 8.0 software. Area under the peak was determined to enable the determination the free ions and contact ions (%), and hence, the percentage of ions could be calculated using the equation below [22]:

$$\text{Percentage of free ions } (\%) = \frac{A_f}{A_f + A_c} \times 100\% \quad (2)$$

where A_f is the area under the peak representing free ions region and A_c is the total area under the peak representing contact ions region. The number of mobile ions (η), ionic mobility (μ) and diffusion coefficient (D) of the SBEs system was calculated using equation [23]:

$$\eta = \frac{MN_A}{V_{Total}} \times \text{free ions}(\%) \quad (3)$$

$$\mu = \frac{\sigma}{\eta e} \quad (4)$$

$$D = \frac{KT\mu}{e} \quad (5)$$

In this work, M is the number moles for each weight percentage of NH_4Br, N_A is Avogadro's number and V_{total} is the total volume of the alginate-NH_4Br SBEs system, e is the electron charge, k is the Boltzmann constant and T is the absolute temperature in kelvin.

Results and discussion

FTIR analysis

Figure 1 depicts the optimization structure of pure alginate with empirical formula of $C_6H_7O_7$ [24, 25]. According to Hema et al. [26], the cations of ammonium salts are expected to coordinate to polar groups of polymer matrix resulting in polymer-ammonium salts complexation. The complexation between alginate and NH_4Br can be shown if any changes in intensity or wavenumber of FTIR spectra are observed. There is possible interaction of alginate at polar groups of carboxylate group (COO^-), hydroxyl group (O–H) and glycoside bond (C–O–C). In Fig. 2, the FTIR spectra of pure alginate show that there are peak characteristics of 1043 cm^{-1}, 1440 cm^{-1}, 1652 cm^{-1}, 3001 cm^{-1} and 3391 cm^{-1} which are attributed to glycoside bond (C–O–C), symmetric stretching of COO^-, asymmetric stretching of COO^-, polymer backbone structure of stretching CH_2 and stretching OH group, respectively [27–31]. Meanwhile, for NH_4Br, the twin stretching peaks at 3105 cm^{-1} and 3200 cm^{-1} correspond to N–H amine group and one absorption peak at 1420 cm^{-1} highlighted as ammonium ion (NH_4^+) functioning as free ions in SBEs system [6, 32, 33].

Figure 3 presents the FTIR spectra for various samples of SBEs system. The vibrational bands at 1043 cm^{-1}, 1440 cm^{-1}, 1625 cm^{-1} and 3391 cm^{-1} correspond to polar group of C–O–C, symmetric COO^-, asymmetric COO^- and –OH, respectively, which are existed in polymer matrix. Based on Fig. 3, the addition of 5 wt. %

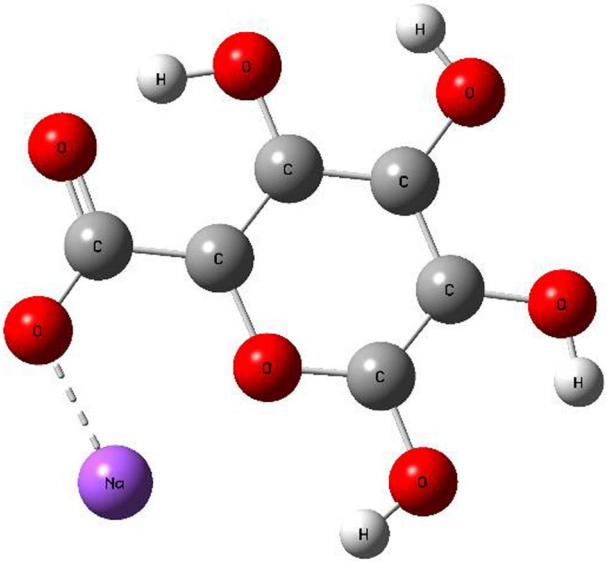

Fig. 1 The optimized structure of pure alginate [3]

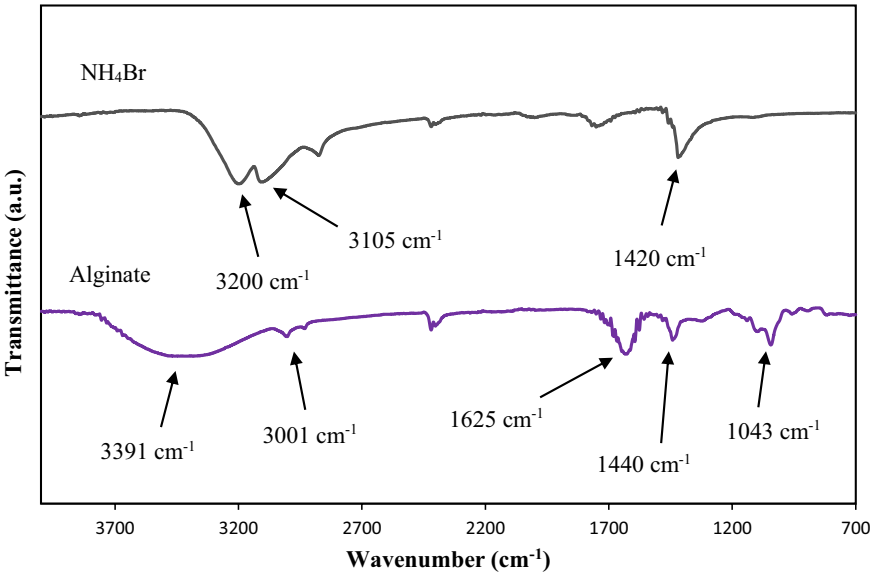

Fig. 2 The FTIR spectrum of pure alginate and NH_4Br

NH_4Br dopant showed the shifted and increase in their intensity for absorption peaks from 1043 cm^{-1} to 1025 cm^{-1} which highlighted as C–O–C stretching vibrations and remain unchanged when added with 15 wt. % NH_4Br. The shifted of IR peak at this band could be due to the migration of NH_4^+ cations toward C–O–C group in

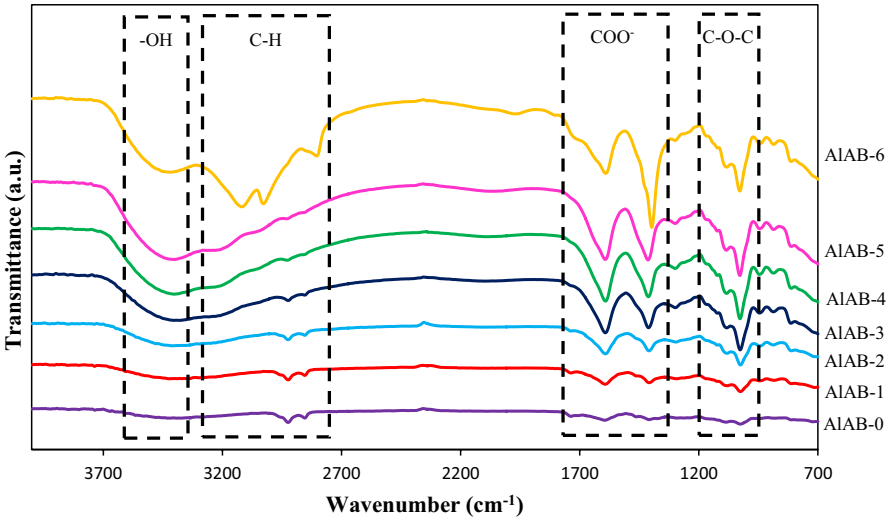

Fig. 3 The FTIR spectrum of alginate-NH_4Br in SBEs system

alginate [4]. The peak spectra at 20 wt. % NH_4Br shifted further to 1029 cm^{-1} due to weak van der Waals attraction of dipole–dipole forces upon the increment of ionic dopant. The change of peak was affected by attraction of the ionic dopant to lone pair electrons of polymer when NH_4Br was added in SBEs system [34, 35].

Notably, the characteristic peak of un-doped sample at 1440 cm^{-1} and 1625 cm^{-1} correspond to symmetric COO^- and asymmetric COO^- are found to shifted to lower value at 1409 cm^{-1} and 1595 cm^{-1} when incorporated with NH_4Br. In the present work, ion conduction is possible occurred based on Grotthuss mechanism due to the proton migration (H^+) in polymer matrix [36]. This mechanism can be explained due to the coordination interaction of (COO^-) moiety of alginate with H^+ ion of [NH_4^+] substructure in NH_4Br, which triggers the protonation between the cation (H^+) and the carboxylate group of alginate via Grotthuss mechanism [37–39]. The increment of ionic dopant also leads to the increasing in peak intensity SBEs system from sample AlAB-1 to AlAB-6. In the present system, NH_4^+ cation moiety functioning as electrophile positive ion in NH_4Br. There is tendency for the interaction between the coordinating site (oxygen) of carboxylate anion from alginate and the NH_4^+ via electrostatic attraction, which lead to the increase in ionic conductivity and electrochemical properties of SBEs system [1, 40]. It can be found there is decrement of peak intensity at 1595 cm^{-1} when introduce NH_4Br more than 20 wt. %, and it is clearly can be seen for sample containing with 30 wt. %. This could be due to the phenomenon so-called salt aggregation where it is expected to decrease the mobility of ions which resulted to the decrement in ionic conductivity [41].

On the other hand, the broadband of pure alginate observed at 3391 cm^{-1} correspond to –OH group shifted to low absorption band at 3389 cm^{-1} upon addition of NH_4Br. The addition of NH_4Br leads to the shifting in wavenumber at –OH group indicating the presence of N–H stretching from NH_4Br [42]. This trend is found

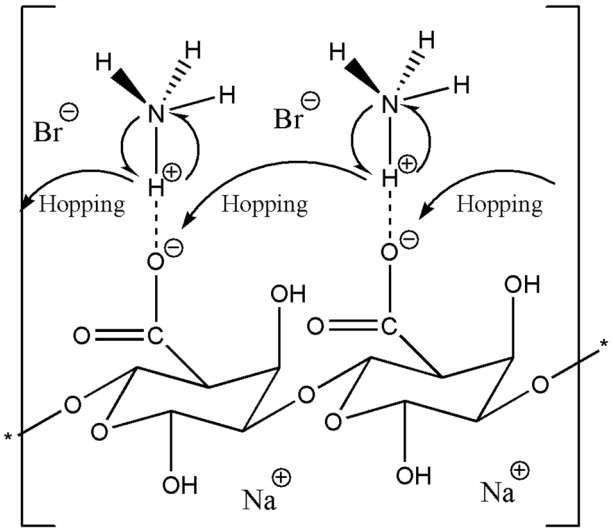

Scheme 1 Schematic diagram of alginate having interacted with NH_4Br salt via [$N–H_4^+$]

Table 2 Summary of complexation between alginate and NH_4Br in SBEs system

Wavenumber (cm^{-1})							Functional group
AlAB-0	AlAB-1	AlAB-2	AlAB-3	AlAB-4	AlAB-5	AlAB-6	
1043	1025	1025	1025	1027	1028	1029	C–O–C stretching
1440	1409	1410	1411	1412	1414	1397	(COO–) symmetric stretching
1625	1595	1593	1593	1592	1592	1591	(COO–) asymmetric stretching
3001	2924	2925	2925	2928	2931	3028	C–H stretching
3391	3389	3414	3403	3403	3404	3416	O–H stretching

to be similar as discovered by other researcher that using NH_4Br as ionic dopant in SBEs system [43]. The schematic diagram showing their possible interaction between alginate and NH_4Br is presented in Scheme 1 and changes of IR-band were summarized in Table 2.

TGA analysis

The thermal properties of alginate-NH_4Br SBEs system were determined using thermal gravimetric analysis (TGA). Figure 4 depicts the thermograms for sample AlAB-0, AlAB-2, AlAB-4 and AlAB-6-based SBEs system. Three distinct decomposition stages were observed in temperature range of 30 °C until 800 °C under N_2 atmosphere and were tabulated in Table 3.

From Fig. 4, the first-stage decomposition in range 170–210 °C is related to losses of moisture content in SBEs system [44, 45]. The minimum weight loss

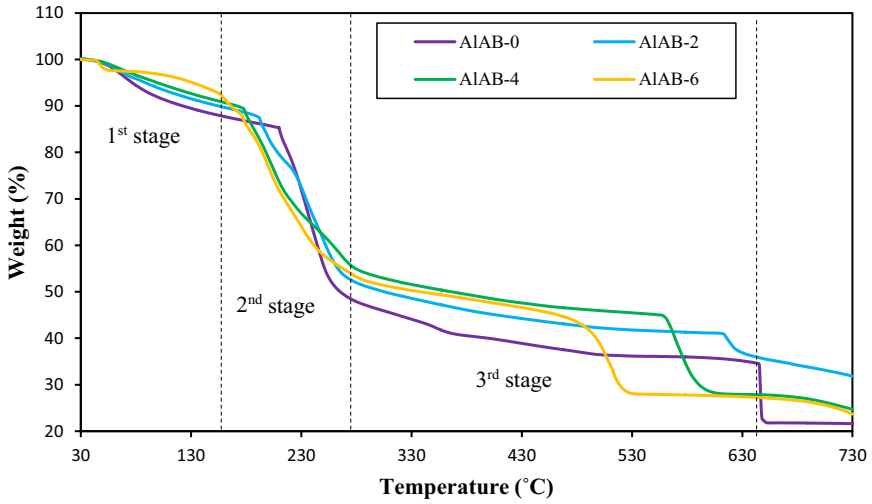

Fig. 4 TGA thermograms of alginate-NH_4Br SBEs system

Table 3 Thermal properties of SBEs system

Sample	Maximum temperature (°C)			Weight loss (Δ%)		
	1st stage	2nd stage	3rd stage	1st stage	2nd stage	3rd stage
AlAB-0	210	270	645	14.69	36.29	14.54
AlAB-2	192	273	613	12.56	34.66	11.84
AlAB-4	178	280	560	11.07	34.12	4.57
AlAB-6	155	278	483	7.22	39.26	10.37

was observed at AlAB-6 with 7.22% compared to un-doped sample (AlAB-0) with 14.09%. According to Ahmad and Isa [46], the temperature at range 50–200 °C attributable to evaporation and degradation process of water and residual solvent inside polymer electrolyte film. The second-stage decomposition was contributed to the loss of carboxylate group (COO^-) from the polymer backbone. The pure alginate (AlAB-0) exhibits weight loss about 36.29% with decomposed temperature 270 °C. According to Swamy and Ramaraj [47], the alginate consists major structure of carboxylate group in polymer matrix and easily to undergo decarboxylation (degradation) at range 219–261 °C. However, addition of ionic dopant into polymer backbone attributed to dissociation easily upon heating process where more protonation of cation (H^+) from NH_4Br to COO^- of alginate backbone as discussed in FTIR analysis; hence, the decomposed temperature increased and the weight loss of SBEs system reduced. The decrement of weight loss in AlAB-4 with 34.12% were expected strong amorphous phase in the structure, which enhance the heat sensitivity of SBEs system. This suggesting

the enhancement of thermal stability where less monomer detached from polymer backbone due to complexation of alginate-NH_4Br in SBEs system [37].

A small reduction of weight loss was observed at last stage of decomposition in range between 280 and 650 °C. AlAB-4 showed minimal value of weight loss 4.57% at temperature 560 °C. Cheong and Zhitomirsky [48] and Huq [49] reported in their work there are degradation and burning out of remaining carbon from alginate polymer when reached ~ 500 °C. The increment of temperature above decomposed temperature 650 °C (prolong heating) resulting the carbonization of polymer backbone into ash formation [50, 51]. From TGA analysis, alginate polymer is suitable used as host in electrochemical devices due to thermal stability in SBEs system.

DSC analysis

Differential scanning calorimetry (DSC) was used to characterize the thermal behavior of materials, which can further confirm the presence of miscibility between alginate and NH_4Br by measures the change in the heat capacity as the polymer matrix goes from the glass state to rubber state as known as T_g [52, 53]. DSC thermograms of the various alginate-NH_4Br SBEs samples were presented in Fig. 5, and the glass transition temperatures (T_g) are depicted by arrows as shown in figure. From Fig. 5a, the T_g for AlAB-0 was not detected at this range of temperature study. However, the exothermic peaks were founded at 180 °C indicates the further process of degradation. According to Báez et al. [54] and Soazo et al. [55], the exothermic peaks observed at temperatures between 170 and 250 °C result from degradation of alginate due to dehydration and depolymerization of the protonated carboxylic groups and oxidation reactions of the macromolecule.

In SBEs system, the T_g value was clearly observed, and the observed T_g depends on the dopant composition. The incorporation of 10 wt. % of NH_4Br to alginate polymer matrix showed the initial T_g value at 77.52 °C due to the formation of coordination between the polymer chain segments and ions formation from ionic dopant which increases the energy barrier to the segmental motion of the polymer chains; thus, the stiffening of the polymer chains may occur [56]. Notably, the addition of 20 wt. % of NH_4Br (AlAB-4) causes the T_g to shift to lower temperature, thus, it helps soften the polymer chain backbone, and this similarly been observed by other research work [57]. The decrease in T_g indicates an increase in the flexibility of alginate chains; hence, the AlAB-4 was expected to exhibit highest ionic conductivity value [4]. Further increase in the composition of NH_4Br leads to the increment of T_g value. It can be attributed to the formation of ion aggregates in alginate polymer matrix, which reduced the flexibility of the polymer chain [58]. A similar trend has been observed by Moniha et al. [59] for the system based on iota carrageenan complexed with ammonium thiocyanate (NH_4SCN).

XRD analysis

Figure 6 depicts the XRD patterns from various NH_4Br compositions doped with alginate as a SBEs system. For un-doped (AlAB-0) sample, it can be observed that

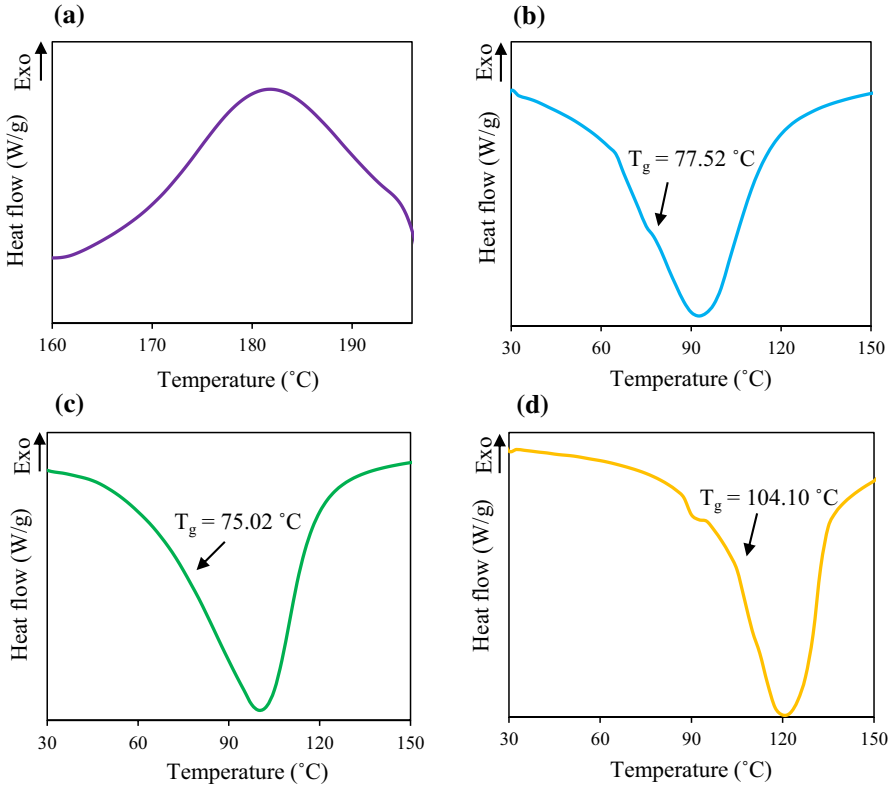

Fig. 5 DSC thermograms of **a** AlAB-0, **b** AlAB-2, **c** AlAB-4 and **d** AlAB-6 SBEs system

there are two principal diffraction peaks at 13.84° and 23.18° revealed the semi-crystalline structure as reported by other works [60, 61]. According to Yang et al. [62] and Zhang et al. [63], the pure alginate showed two broad amorphous peaks attributed to typical polysaccharides which as similarly observed in the present system for the un-doped (AlAB-0) sample.

As stated by Hodge et al. [64–66] criterion, the amorphous nature of polymer matrix can be established by a correlation between the height of the peak intensity and degree of crystallinity. It clearly can be seen that the addition of NH_4Br reducing the intensity of broad peak and shifted to higher angle from sample AlAB-1 until AlAB-4. Disappearance of sharp peaks inferred that the dopant systems are completely dissociate in the polymer matrix [13]. This indicates there are complexation occur between NH_4Br and alginate polymer resulting in increment of amorphous hump [36]. The maximum amorphous nature of polymer membrane eases the protonation of H^+ to the alginate backbone by imparts more oxygen vacant site and thereby improve the ionic conductivity to the greater extent [67–69]. Based on XRD results, it shown that the AlAB-4 sample exhibits good amorphous in nature and no noticeable peaks founded in system which expected to achieve higher ionic

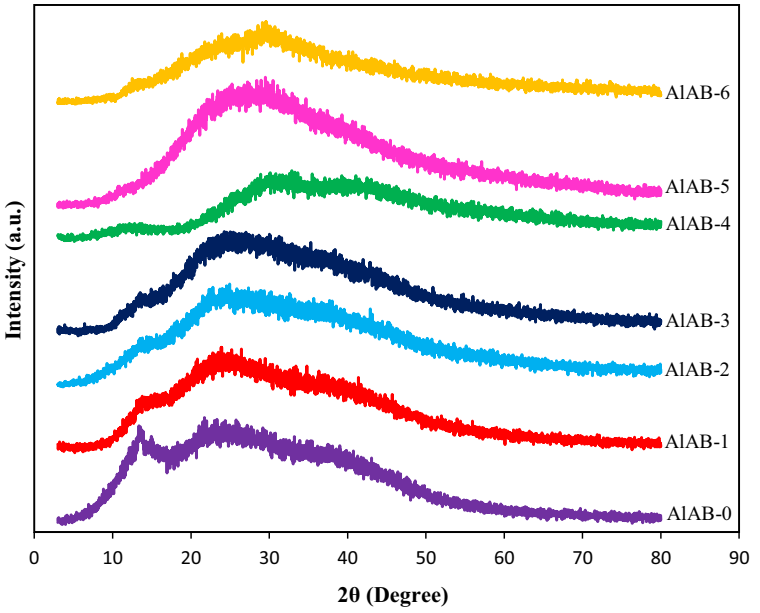

Fig. 6 X-ray diffractogram of all alginate-NH_4Br SBEs system

conductivity. However, the amorphous phase of SBEs system starts to decrease at sample AlAB-5, and this might be due to incapable of host polymer (alginate) to accommodate the NH_4Br which leads to decrease in transport properties values and ionic conductivity [70, 71].

SEM analysis

Scanning electron microscopy (SEM) was carried out for extensive morphological inspection of cross section in alginate-NH_4Br SBEs film. The surface morphology for SBEs system with the magnification of 2000 times and range 50 µm was depicted in Fig. 7. From the SEM image of alginate film (AlAB-0), it was found that the structure was smooth surface with no phase separation, suggesting no susceptible filling [72].

In the SBEs system, AlAB-2 showed no differences in the surface properties implying that the samples are homogeneous and amorphous nature. Due to the complete dissolution of salt in polymer matrix, the enhancement of segmental motion takes place in the polymer electrolyte. Such segmental motion produces empty spaces, which enables the easy flow of ions in the material in the presence of electric field, and it expected increases the ionic conductivity [73]. Upon addition of salt until sample AlAB-4, the SEM image showed the homogeneity rough surface without any phase separation that could be due to the ion set-ups in the polymer electrolyte which enhanced the transport of protonation [74]. However, addition 30 wt% of NH_4Br into the alginate led to the formation of salt agglomeration. The results

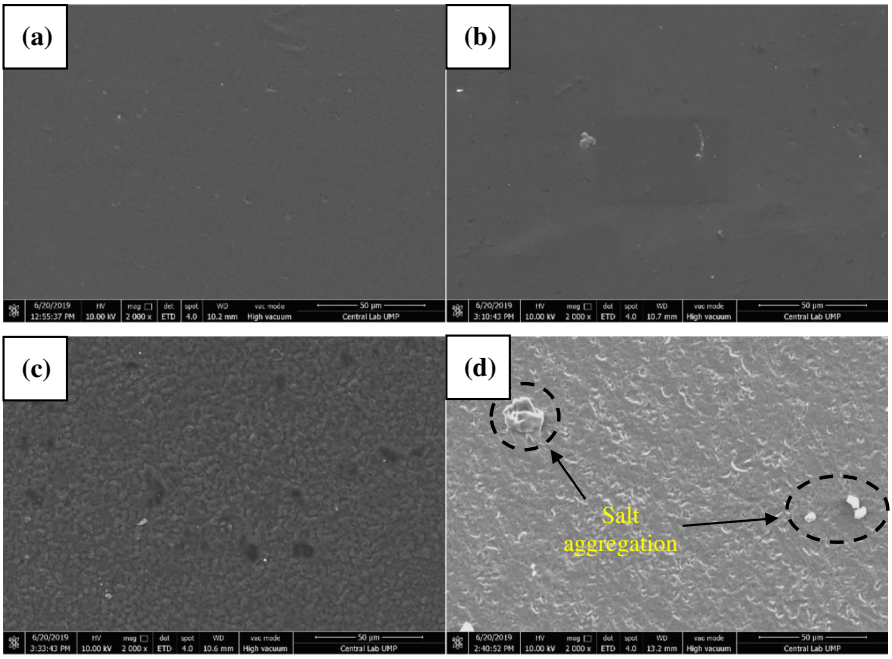

Fig. 7 Surface micrographs for **a** AlAB-0, **b** AlAB-2, **c** AlAB-4 and **d** AlAB-6 of alginate-NH_4Br SBEs system

shown that the morphology of samples were found to aligned with XRD analysis where it might be formed by less dissolution of salt in the polymer matrix.

Conductivity analysis

Figure 8 depicts ionic conductivity value for various compositions of NH_4Br SBEs system at ambient temperature (303 K). The conductivity value for un-doped (AlAB-0) sample was observed to be 4.67×10^{-7} S cm^{-1}. It can be clearly seen that the ionic conductivity begins to increase when 5 wt. % of NH_4Br was added and achieved to the optimum value at 4.41×10^{-5} S cm^{-1} for sample AlAB-04. The enhancement of ionic conductivity to the higher value could be attributed to the increment in amorphous phase in SBEs system as observed from XRD analysis, thus, large amount of H^+ can migrate toward the coordinating site in biopolymer host with lesser of blocking pathway [75, 76]. According to Rasali and Samsudin [77], the increment of ionic conductivity proved the increasing number of mobile ions that led to interaction between salt and polymer matrix via Grotthuss mechanism. However, the addition of salt beyond 20 wt. % depicts the decrement of ionic conductivity in SBEs system. This attributes to the re-crystallization of polymer matrix where packed with ions (salt aggregation) as demonstrated in XRD and SEM analysis; thus leads to the enhancement of energy barriers to segmental motion in SBEs system [78].

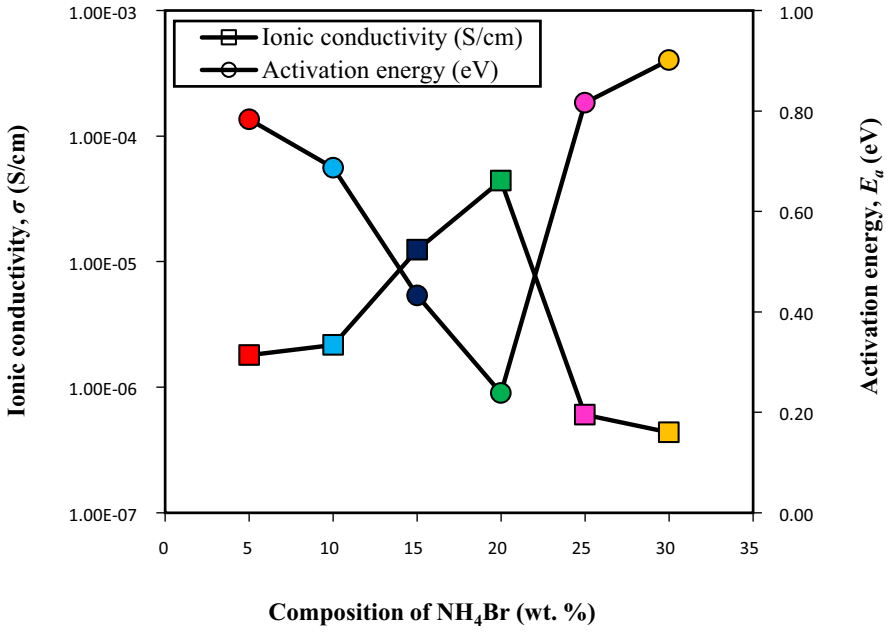

Fig. 8 Ionic conductivity and activation energy for alginate-NH_4Br SBEs system at ambient temperature

The temperature-dependence study of ionic conductivity for various alginate-NH_4Br SBEs at different temperature range from 303 to 353 K was presented in Fig. 9. In this study, it can be observed that the ionic conductivity of SBEs system increased with temperature, and this indicates that the polymer electrolyte is thermally activated [79]. This can be proved as revealed by TGA analysis where the polymer backbone (alginate) has been improvised with addition of NH_4Br in alginate and led to expansion of biopolymer matrix to provided free volume where the ions easily to migrate, thus resulting in increment of conductivity value [80, 81]. All SBEs system obeys the Arrhenius behavior where regression value, R^2 close to unity ($R^2 \sim 1$) [82, 83]. The activation energy (E_a) for the SBEs system has been calculated by the linear fitting of the Arrhenius equation [84, 85].

$$\sigma = \sigma_0 \exp\left(-\frac{E_a}{kT}\right) \tag{6}$$

where is a σ_0 pre-exponential factor, E_a is the activation energy of electrical conduction, k is the Boltzmann constant and T is the temperature in Kelvin. From Fig. 8, it can be seen that the activation energy reduces as the ionic conductivity increases. The highest conducting sample (AlAB-4) with conductivity 4.41×10^{-5} S cm^{-1} exhibits lowest activation energy of 0.2382 eV. This phenomenon generates faster rate of H^+ motion in polymer chain where it leads to enhancement of amorphous phase and higher in ionic conductivity for the present SBEs system [86]. Therefore,

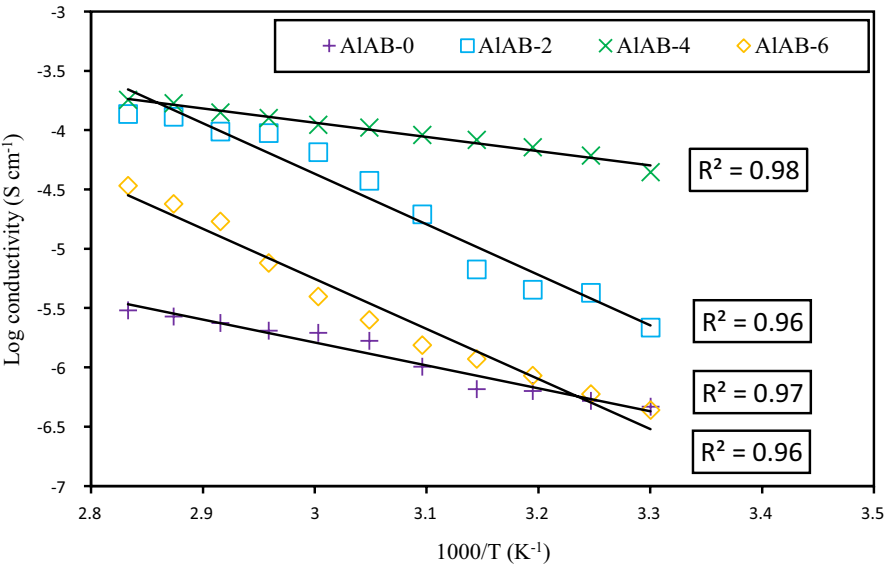

Fig. 9 Ionic conductivity of alginate-NH_4Br SBEs system at selected temperature

the H^+ ions required less energy to migrate to coordinating site of polymer matrix [87].

Transport analysis

In the present system, the transport parameter was determined using FTIR deconvolution technique, which is favorable method [88–90]. FTIR deconvolution for sample AlAB-3, AlAB-4 and AlAB-6 of SBEs system was presented in Fig. 10. The range of wavenumber between 1300 cm^{-1} and 1500 cm^{-1} is selected due to the most significant changes of IR-band peak and wavenumber as shown from FTIR analysis. The peaks at ~ 1410 cm^{-1} are assigned as free ions and peaks at ~ 1400 cm^{-1} and ~ 1463 cm^{-1} assigned as contact ion pairs and formation ion aggregates, respectively [91, 92]. Based on deconvolution approach, the percentage of free ions and contact ions was calculated using Eq. 2 and tabulated in Table 4. It can be observed that the free ions increase with addition of NH_4Br until reached sample AlAB-4. This attributes to increment of ion dissociation from NH_4^+ to polymer matrix; thus, it directly increases the conductivity value of SBEs system [36], whereas at AlAB-5, the free ions start to decrease slightly which is due to the re-association of ions, therefore lead to the formation of ion cluster and the decrement of amorphous phase (as shown in XRD and SEM analysis) [90, 93].

Based on the parameters in Table 4, number of mobile ions, (η), ionic mobility (μ) and diffusion coefficient (D) were calculated. It is clearly can be seen that the number of mobile ions increased linearly with addition of NH_4Br; meanwhile the ionic mobility and diffusion coefficient followed the conductivity pattern where the

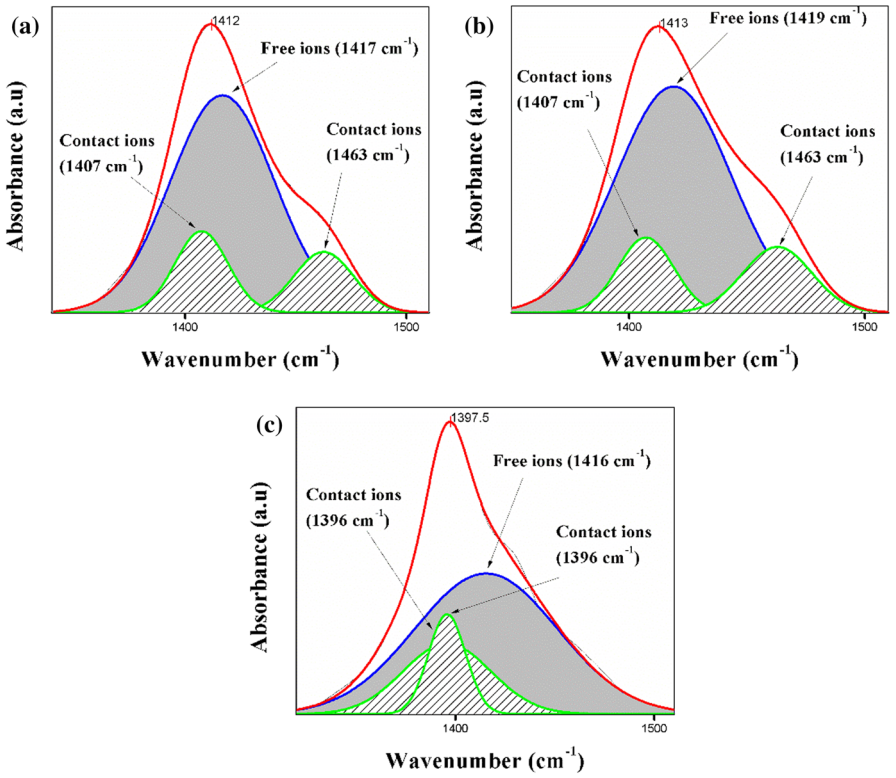

Fig. 10 FTIR deconvolution for sample **a** AlAB-3 **b** AlAB-4 and **c** AlAB-6 SBEs system

Table 4 Transport properties of alginate-NH_4Br SBEs system

Sample	Free ions (%)	Contact ions (%)	Num. of mobile ions, η (cm^{-3})	Ionic mobility, μ ($cm^2\ V^{-1}\ s^{-1}$)	Diffusion coefficient, D ($cm^2\ s^{-1}$)
AlAB-2	72.34	27.66	9.55×10^{22}	1.42×10^{-10}	3.70×10^{-12}
AlAB-3	74.07	25.93	1.48×10^{23}	5.26×10^{-10}	1.37×10^{-11}
AlAB-4	75.02	24.98	2.01×10^{23}	1.37×10^{-9}	3.58×10^{-11}
AlAB-5	71.75	28.25	2.42×10^{23}	1.56×10^{-11}	4.06×10^{-13}
AlAB-6	66.94	33.06	2.73×10^{23}	1.00×10^{-11}	2.61×10^{-13}

highest μ and D for AlAB-4 is 1.37×10^{-9} $cm^2\ V^{-1}\ s^{-1}$ and 3.58×10^{-11} $cm^2\ s^{-1}$, respectively. Similar pattern was reported by Ramlli and Isa [89] where the ionic mobility (μ) and diffusion coefficient (D) were governed by ionic conductivity in their polymer electrolyte system. The continuous increment of η with addition of NH_4Br exhibits the over crowd of H^+ ions which lead to formation of ion cluster [94]. Therefore, ions migration requires higher activation energy, E_a to undergo protonation process; thus, the μ, D and ionic conductivity value start to reduce rapidly

in SBEs system [23]. The increase in ionic dopant altered the dipole interaction of H^+ ions in alginate-NH_4Br complexes and promoted the re-crystallization structure as proven by XRD analysis [36].

Conclusion

In the present work, solid biopolymer electrolytes (SBEs) system based on alginate polymer doped with various compositions of ionic dopant NH_4Br was prepared via solution casting technique. The complexation between alginate and NH_4Br was investigated by using FTIR analysis where there are significant possible interaction happen at C–O–C stretching, symmetric and asymmetric COO^- stretching and OH^- stretching. There is strong contribution of hydrogen bonding from protonation H^+ to COO^- moiety of alginate polymer. The TGA and DSC analysis shown the SBEs system promoted good thermal stability where also improved their amorphous phase as revealed by XRD and SEM analysis. The highest ionic conductivity at ambient temperature was observed for sample AlAB-4 with 4.41×10^{-5} S cm^{-1}. The temperature-dependence ionic conductivity of present all SBEs system obey the Arrhenius behavior where the regression value, R^2 close to unity ($R^2 \sim 1$) and thermally assisted. The ionic conductivity of alginate-NH_4Br SBEs system was found to be governed by the ionic mobility (μ) and diffusion coefficient (D). From the results obtained, it shown that the present SBEs system-based alginate-NH_4Br has the possible potential to be applied for electrochemical applications.

Acknowledgements The authors would like to thank MOHE for FRGS (RDU1901114) and (RDU170115), UMP for internal grant RDU1703189, Faculty of Industrial Sciences & Technology, Universiti Malaysia Pahang, for the help and support given for the completion of this work. The authors would also like to thank members of Ionic Materials Team, which are N.M.J. Rasali, M.A. Saadiah and N.F. Mazuki for kindly help in completing this research.

References

1. Monisha S, Mathavan T, Selvasekarapandian S, Benial AMF, Aristatil G, Mani N, Premalatha M (2017) Investigation of bio polymer electrolyte based on cellulose acetate-ammonium nitrate for potential use in electrochemical devices. Carbohydr Polym 157:38–47
2. Tan G, Wu F, Zhan C, Wang J, Mu D, Lu J, Amine K (2016) Solid-state li-ion batteries using fast, stable, glassy nanocomposite electrolytes for good safety and long cycle-life. Nano Lett 16(3):1960–1968
3. Sohaimy MIH, Isa MIN (2017) Ionic conductivity and conduction mechanism studies on cellulose based solid polymer electrolytes doped with ammonium carbonate. Polym Bull 74(4):1371–1386
4. Rasali NMJ, Nagao Y, Samsudin AS (2019) Enhancement on amorphous phase in solid biopolymer electrolyte based alginate doped NH_4NO_3. Ionics 25(2):641–654
5. Samsudin AS, Kuan ECH, Isa MIN (2011) Investigation of the potential of proton-conducting biopolymer electrolytes based methyl cellulose-glycolic acid. Int J Polym Anal Charact 16(7):477–485
6. Ahmad NH, Isa MIN (2015) Structural and ionic conductivity studies of CMC based polymerelectrolyte doped with NH_4Cl. Adv Mater Res 1107:247–252
7. Shukur MF, Kadir MFZ (2015) Hydrogen ion conducting starch-chitosan blend based electrolyte for application in electrochemical devices. Electrochim Acta 158:152–165

8. Chappalwar T, Ojha S (2018) Shelf life enhancement of muscle foods with biodegradable film packaging. J Anim Feed Sci Technol 6(33):39
9. Kumar R, Sharma RK, Singh AP (2018) Grafted cellulose: a bio-based polymer for durable applications. Polym Bull 75(5):2213–2242
10. Rosli NHA, Noor SAM, Ahmad KA, Winie T (2017) Effect of HNO_3 on structual and electrical properties of hexanoyl chitosan/polystrene-$LICF_3SO_3$-TIO_2. J Fundam Appl Sci 9(3S):141–153
11. Samsudin AS, Isa MIN, Mohamad N (2011) New types of biopolymer electrolytes: ionic conductivity study on CMC doped with NH_4Br. J Curr Eng Res 1(1):7–11
12. Shukur MF, Kadir MFZ (2015) Electrical and transport properties of NH_4Br-doped cornstarch-based solid biopolymer electrolyte. Ionics 21(1):111–124
13. Karthikeyan S, Selvasekarapandian S, Premalatha M, Monisha S, Boopathi G, Aristatil G, Arun A, Madeswaran S (2017) Proton-conducting I-Carrageenan-based biopolymer electrolyte for fuel cell application. Ionics 23(10):2775–2780
14. Vahini M, Muthuvinayagam M (2018) AC impedance studies on proton conducting biopolymer electrolytes based on pectin. Mater Lett 218:197–200
15. Singh R, Bhattacharya B, Tomar SK, Singh V, Singh PK (2017) Electrical, optical and electrophotochemical studies on agarose based biopolymer electrolyte towards dye sensitized solar cell application. Measurement 102:214–219
16. Rahmani V, Sheardown H (2018) Protein-alginate complexes as pH-/ion-sensitive carriers of proteins. Int J Pharm 535(1–2):452–461
17. Obot IB, Onyeachu IB, Kumar AM (2017) Sodium alginate: a promising biopolymer for corrosion protection of API X60 high strength carbon steel in saline medium. Carbohydr Polym 178:200–208
18. Merakchi A, Bettayeb S, Drouiche N, Adour L, Lounici H (2019) Cross-linking and modification of sodium alginate biopolymer for dye removal in aqueous solution. Polym Bull 76(7):3535–3554
19. Gondaliya N, Kanchan DK, Sharma P, Joge P (2011) Structural and conductivity studies of poly (ethylene oxide)–silver triflate polymer electrolyte system. Mater Sci Appl 2(11):1639
20. Ahmad NH, Bakar NY, Isa MIN (2017) Structural and ionic conductivity studies on proton conducting solid biopolymer electrolyte based on 2hydroxyethyl cellulose incorporated DTAB. In: AIP conference proceedings, vol 1. AIP Publishing, p 020080
21. Wu X, Xu Y, Jiang H, Wei Z, Hong JJ, Hernandez AS, Du F, Ji X (2018) NH_4^+ topotactic insertion in Berlin green: an exceptionally long-cycling cathode in aqueous ammonium-ion batteries. ACS Appl Energy 1(7):3077–3083
22. Zainuddin NK, Rasali NMJ, Samsudin AS (2018) Study on the effect of PEG in ionic transport for CMC-NH_4Br-based solid polymer electrolyte. Ionics 24(10):3039–3052
23. Chai MN, Isa MIN (2016) Novel proton conducting solid bio-polymer electrolytes based on carboxymethyl cellulose doped with oleic acid and plasticized with glycerol. Sci Rep 6:27328
24. Rameshbabu N, Kumar TSS, Rao KP (2010) Influence of microwave power, irradiation time and polymeric additions on synthesis of nanocrystalline hydroxyapatite. Mater Res Innov 14(1):45–50
25. Parvin F, Yeasmin F, Islam JMM, Molla E, Khan MA (2013) Effect of gamma irradiated sodium alginate on Malabar spinach (*Basella alba*) and spinach (*Spinacia oleracea*) as plant growth promoter. Am Acad Sch Res J 5(5):63
26. Hema M, Selvasekerapandian S, Hirankumar G, Sakunthala A, Arunkumar D, Nithya H (2009) Structural and thermal studies of PVA: NH_4I. J Phys Chem Solids 70(7):1098–1103
27. Aprilliza M (2017) Characterization and properties of sodium alginate from brown algae used as an ecofriendly superabsorbent. In: IOP conference series: materials science and engineering, vol 1. IOP Publishing, p 012019
28. Zhang N, Xu J, Gao X, Fu X, Zheng D (2017) Factors affecting water resistance of alginate/gellan blend films on paper cups for hot drinks. Carbohydr Polym 156:435–442
29. Treenate P, Monvisade P (2017) In vitro drug release profiles of pH-sensitive hydroxyethylacryl chitosan/sodium alginate hydrogels using paracetamol as a soluble model drug. Int J Biol Macromol 99:71–78
30. Fawzy MA, Gomaa M, Hifney AF, Abdel-Gawad KM (2017) Optimization of alginate alkaline extraction technology from *Sargassum latifolium* and its potential antioxidant and emulsifying properties. Carbohydr Polym 157:1903–1912
31. Tong Z, Chen Y, Liu Y, Tong L, Chu J, Xiao K, Zhou Z, Dong W, Chu X (2017) Preparation, characterization and properties of alginate/poly (γ-glutamic acid) composite microparticles. Mar Drugs 15(4):91

32. Ramlli MA, Kamarudin KH, Isa MIN (2015) Ionic conductivity and structural analysis of carboxymethyl cellulose doped with ammonium fluoride as solid biopolymer electrolytes. Am-Eurasian J Sustain Agric 46–52
33. Ahmad NH, Isa MIN (2015) Proton conducting solid polymer electrolytes based carboxymethyl cellulose doped ammonium chloride: ionic conductivity and transport studies. Int J Plast Technol 19(1):47–55
34. Samsudin AS, Khairul WM, Isa MIN (2012) Characterization on the potential of carboxy methylcellulose for application as proton conducting biopolymer electrolytes. J Non-Cryst Solids 358(8):1104–1112
35. Kadir MFZ, Salleh NS, Hamsan MH, Aspanut Z, Majid NA, Shukur MF (2018) Biopolymeric electrolyte based on glycerolized methyl cellulose with NH_4Br as proton source and potential application in EDLC. Ionics 24(6):1651–1662
36. Zainuddin NK, Samsudin AS (2018) Investigation on the effect of NH_4Br at transport properties in K–carrageenan based biopolymer electrolytes via structural and electrical analysis. Mater Today Comm 14:199–209
37. Samsudin AS, Lai HM, Isa MIN (2014) Biopolymer materials based carboxymethyl cellulose as a proton conducting biopolymer electrolyte for application in rechargeable proton battery. Electrochim Acta 129:1–13
38. Wei J (2019) Proton-conducting materials used as polymer electrolyte membranes in fuel cells. In: Song K, Liu C, Guo JZ (eds) Polymer-based multifunctional nanocomposites and their applications. Elsevier, Amsterdam, pp 245–260
39. Miyake T, Rolandi M (2017) Grotthuss mechanism: from proton transport in ion channels to bioprotonic devices. In: Irimia-Vladu M, Glowacki ED, Sariciftci NS, Bauer S (eds) Green materials for electronics. Wiley, Hoboken
40. Bakhtin S, Shved E, Bespal'ko Y (2017) Nucleophile-electrophile interactions in the reaction of oxiranes with carboxylic acids in the presence of tertiary amines. J Phys Org Chem 30(12):e3717
41. Rasali NMJ, Samsudin AS (2018) Ionic transport properties of protonic conducting solid biopolymer electrolytes based on enhanced carboxymethyl cellulose-NH_4Br with glycerol. Ionics 24(6):1639–1650
42. Fu G, Dempsey J, Izaki K, Adachi K, Tsukahara Y, Kyu T (2017) Highly conductive solid polymer electrolyte membranes based on polyethylene glycol-bis-carbamate dimethacrylate networks. J Power Sources 359:441–449
43. Mazuki NF, Fuzlin AF, Saadiah MA, Samsudin AS (2019) An investigation on the abnormal trend of the conductivity properties of CMC/PVA-doped NH_4Cl-based solid biopolymer electrolyte system. Ionics 25(6):2657–2667
44. Rikukawa M, Sanui K (2000) Proton-conducting polymer electrolyte membranes based on hydrocarbon polymers. Prog Polym Sci 25(10):1463–1502
45. Liew C-W, Ramesh S (2013) Studies on ionic liquid-based corn starch biopolymer electrolytes coupling with high ionic transport number. Cellulose 20(6):3227–3237
46. Ahmad NH, Isa MIN (2016) Characterization of un-plasticized and propylene carbonate plasticized carboxymethyl cellulose doped ammonium chloride solid biopolymer electrolytes. Carbohydr Polym 137:426–432
47. Swamy TMM, Ramaraj B, Lee JH (2008) Sodium alginate and its blends with starch: thermal and morphological properties. J Appl Polym Sci 109(6):4075–4081
48. Cheong M, Zhitomirsky I (2008) Electrodeposition of alginic acid and composite films. Colloids Surf A 328(1–3):73–78
49. Huq T, Salmieri S, Khan A, Khan RA, Le Tien C, Riedl B, Fraschini C, Bouchard J, Uribe-Calderon J, Kamal MR (2012) Nanocrystalline cellulose (NCC) reinforced alginate based biodegradable nanocomposite film. Carbohydr Polym 90(4):1757–1763
50. Liew C-W, Ramesh S, Arof AK (2014) A novel approach on ionic liquid-based poly (vinyl alcohol) proton conductive polymer electrolytes for fuel cell applications. Int J Hydrogen Energy 39(6):2917–2928
51. Ma X-H, Xu Z-L, Liu Y, Sun D (2010) Preparation and characterization of PFSA–PVA–SiO_2/PVA/PAN difunctional hollow fiber composite membranes. J Membr Sci 360(1–2):315–322
52. Li X, Xie H, Lin J, Xie W, Ma X (2009) Characterization and biodegradation of chitosan–alginate polyelectrolyte complexes. Polym Degrad Stab 94(1):1–6
53. Perumal P, Selvin PC, Selvasekarapandian S (2018) Characterization of biopolymer pectin with lithium chloride and its applications to electrochemical devices. Ionics 24(10):3259–3270

54. Báez GD, Piccirilli GN, Ballerini GA, Frattini A, Busti PA, Verdini RA, Delorenzi NJ (2017) Physicochemical characterization of a heat treated calcium alginate dry film prepared with chicken stock. J Food Sci 82(4):945–951
55. Soazo M, Báez G, Barboza A, Busti PA, Rubiolo A, Verdini R, Delorenzi NJ (2015) Heat treatment of calcium alginate films obtained by ultrasonic atomizing: physicochemical characterization. Food Hydrocolloids 51:193–199
56. Sampathkumar L, Selvin PC, Selvasekarapandian S, Perumal P, Chitra R, Muthukrishnan M (2019) Synthesis and characterization of biopolymer electrolyte based on tamarind seed polysaccharide, lithium perchlorate and ethylene carbonate for electrochemical applications. Ionics 25(3):1067–1082
57. Sikkanthar S, Karthikeyan S, Selvasekarapandian S, Pandi DV, Nithya S, Sanjeeviraja C (2015) Electrical conductivity characterization of polyacrylonitrile-ammonium bromide polymer electrolyte system. J Solid State Electrochem 19(4):987–999
58. Kadir MFZ, Hamsan MH (2018) Green electrolytes based on dextran-chitosan blend and the effect of NH_4SCN as proton provider on the electrical response studies. Ionics 24(8):2379–2398
59. Moniha V, Alagar M, Selvasekarapandian S, Sundaresan B, Hemalatha R, Boopathi G (2018) Synthesis and characterization of bio-polymer electrolyte based on iota-carrageenan with ammonium thiocyanate and its applications. J Solid State Electrochem 22(10):3209–3223
60. Iwaki YO, Escalona MH, Briones JR, Pawlicka A (2012) Sodium alginate-based ionic conducting membranes. Mol Cryst Liq Cryst 554(1):221–231
61. Manjuladevi R, Selvin PC, Selvasekarapandian S, Shilpa R, Moniha V (2018) Lithium ion conducting biopolymer electrolyte based on pectin doped with Lithium nitrate. In: AIP conference proceedings, vol 1. AIP Publishing, p 140075
62. Yang J-M, Wang N-C, Chiu H-C (2014) Preparation and characterization of poly (vinyl alcohol)/sodium alginate blended membrane for alkaline solid polymer electrolytes membrane. J Membr Sci 457:139–148
63. Zhang Y, Wang C, Liu Y, Jiang W, Han G (2019) Preparation and characterization of composite scaffold of alginate and cellulose nanofiber from ramie. Text Res J 89(16):3260–3268
64. Hodge RM, Edward GH, Simon GP (1996) Water absorption and states of water in semicrystalline poly (vinyl alcohol) films. Polymer 37(8):1371–1376
65. Basha SKS, Rao MC (2018) Spectroscopic and electrochemical properties of PVP based polymer electrolyte films. Polym Bull 75(8):3641–3666
66. Basha SKS, Sundari GS, Kumar KV, Rao MC (2018) Preparation and dielectric properties of PVP-based polymer electrolyte films for solid-state battery application. Polym Bull 75(3):925–945
67. Kumar LS, Selvin PC, Selvasekarapandian S, Manjuladevi R, Monisha S, Perumal P (2018) Tamarind seed polysaccharide biopolymer membrane for lithium-ion conducting battery. Ionics 24(12):3793–3803
68. Boopathi G, Pugalendhi S, Selvasekarapandian S, Premalatha M, Monisha S, Aristatil G (2017) Development of proton conducting biopolymer membrane based on agar–agar for fuel cell. Ionics 23(10):2781–2790
69. Hafiza MN, Isa MIN (2017) Solid polymer electrolyte production from 2-hydroxyethyl cellulose: effect of ammonium nitrate composition on its structural properties. Carbohydr Polym 165:123–131
70. Kadir MFZ, Majid SR, Arof AK (2010) Plasticized chitosan–PVA blend polymer electrolyte based proton battery. Electrochim Acta 55(4):1475–1482
71. Monisha S, Mathavan T, Selvasekarapandian S, Benial AMF (2017) Preparation and characterization of cellulose acetate and lithium nitrate for advanced electrochemical devices. Ionics 23(10):2697–2706
72. Alboofetileh M, Rezaei M, Hosseini H, Abdollahi M (2018) Morphological, physico-mechanical, and antimicrobial properties of sodium alginate-montmorillonite nanocomposite films incorporated with marjoram essential oil. J Food Process Preserv 42(5):e13596
73. Sundaramahalingam K, Muthuvinayagam M, Nallamuthu N, Vanitha D, Vahini M (2019) Investigations on lithium acetate-doped PVA/PVP solid polymer blend electrolytes. Polym Bull 76(11):5577–5602
74. Kadir MFZ, Aspanut Z, Yahya R, Arof AK (2011) Chitosan–PEO proton conducting polymer electrolyte membrane doped with NH_4NO_3. Mater Res Innov 15(sup2):s164–s167
75. Rani MSA, Ahmad A, Mohamed NS (2018) A comprehensive investigation on electrical characterization and ionic transport properties of cellulose derivative from kenaf fibre-based biopolymer electrolytes. Polym Bull 75(11):5061–5074

76. Saadiah MA, Zhang D, Nagao Y, Muzakir SK, Samsudin AS (2019) Reducing crystallinity on thin film based CMC/PVA hybrid polymer for application as a host in polymer electrolytes. J Non-Cryst Solids 511:201–211
77. Rasali NMJ, Samsudin AS (2018) Characterization on ionic conductivity of solid bio-polymer electrolytes system based alginate doped ammonium nitrate via impedance spectroscopy. In: AIP conference proceedings, vol 1. AIP Publishing, p 020224
78. Fuzlin AF, Rasali NMJ, Samsudin AS (2018) Effect on Ammonium Bromide in dielectric behavior based Alginate Solid Biopolymer electrolytes. In: IOP conference series: materials science and engineering, vol 1. IOP Publishing, p 012080
79. Perumal P, Selvasekarapandian S, Abhilash KP, Sivaraj P, Hemalatha R, Selvin PC (2019) Impact of lithium chlorate salts on structural and electrical properties of natural polymer electrolytes for all solid state lithium polymer batteries. Vacuum 159:277–281
80. Sundaramahalingam K, Vanitha D, Nallamuthu N, Manikandan A, Muthuvinayagam M (2018) Electrical properties of lithium bromide poly ethylene oxide/poly vinyl pyrrolidone polymer blend elctrolyte. Physica B: Condens Matter 553:120–126
81. Kalaiselvimary J, Prabhu MR (2019) Fabrications and investigation of physicochemical and electrochemical properties of heteropoly acid-doped sulfonated chitosan-based polymer electrolyte membranes for fuel cell applications. Polym Bull 76(3):1401–1422
82. Saadiah MA, Samsudin AS (2018) Study on ionic conduction of solid bio-polymer hybrid electrolytes based carboxymethyl cellulose (CMC)/polyvinyl alcohol (PVA) doped NH_4NO_3. In: AIP conference proceedings, vol 1. AIP Publishing, p 020223
83. Fuzlin AFA, Ismail NS, Nagao Y, Samsudin AS (2019) Electrical properties of a novel solid biopolymer electrolyte based on algi-nate incorporated with citric acid. Makara J Technol 23(1):48–52
84. Mazuki NF, Rasali NMJ, Saadiah MA, Samsudin AS (2018) Irregularities trend in electrical conductivity of CMC/PVA-NH_4Cl based solid biopolymer electrolytes. In: AIP conference proceedings, vol 1. AIP Publishing, p 020221
85. Kurapati S, Gunturi SS, Nadella KJ, Erothu H (2019) Novel solid polymer electrolyte based on PMMA: CH_3COOLi effect of salt concentration on optical and conductivity studies. Polym Bull 76(10):5463–5481
86. Shukur MF, Ithnin R, Illias HA, Kadir MFZ (2013) Proton conducting polymer electrolyte based on plasticized chitosan–PEO blend and application in electrochemical devices. Opt Mater 35(10):1834–1841
87. Samsudin AS, Isa MIN (2012) Structural and ionic transport study on CMC doped NH_4Br: a new types of biopolymer electrolytes. J Appl Sci 12(2):174–179
88. Zainuddin NK, Saadiah MA, Abdul Majeed APP, Samsudin AS (2018) Characterization on conduction properties of carboxymethyl cellulose/kappa carrageenan blend-based polymer electrolyte system. Int J Polym Anal Charact 23(4):321–330
89. Ramlli MA, Isa MIN (2016) Structural and ionic transport properties of protonic conducting solid biopolymer electrolytes based on Carboxymethyl cellulose doped with ammonium fluoride. J Phys Chem B 120(44):11567–11573
90. Ramlli MA, Bashirah NAA, Isa MIN (2018) Ionic conductivity and structural analysis of 2-hyroxyethyl cellulose doped with glycolic acid solid biopolymer electrolytes for solid proton battery. In: IOP conference series: materials science and engineering, vol 1. IOP Publishing, p 012038
91. Woo HJ, Majid SR, Arof AK (2011) Conduction and thermal properties of a proton conducting polymer electrolyte based on poly (ε-caprolactone). Solid State Ionics 199:14–20
92. Majid SR, Arof AK (2007) Electrical behavior of proton-conducting chitosan-phosphoric acid-based electrolytes. Physica B: Condens Matter 390(1–2):209–215
93. Fuzlin AF, Nagao Y, Misnon II, Samsudin AS (2019) Studies on structural and ionic transport in biopolymer electrolytes based on alginate-LiBr. Ionics 26:1923–1938
94. Ramesh S, Ng KY (2009) Characterization of polymer electrolytes based on high molecular weight PVC and Li_2SO_4. Curr Appl Phys 9(2):329–332